

Strain distribution in epitaxial SrTiO_3 thin films

Z. Y. Zhai, X. S. Wu,^{a)} and Z. S. Jiang

National Laboratory of Solid State Microstructures, Nanjing University, Nanjing 210093, China
and Department of Physics, Nanjing University, Nanjing 210093, China

J. H. Hao^{b)}

Department of Applied Physics, The Hong Kong Polytechnic University, Hung Hom, Hong Kong, China

J. Gao

Department of Physics, The University of Hong Kong, Pokfulam Road, Hong Kong, China

Y. F. Cai and Y. G. Pan

Department of Geography, Nanjing University, Nanjing 210093, China

(Received 18 July 2006; accepted 21 November 2006; published online 27 December 2006)

The lattice strain distributions of epitaxial SrTiO_3 films deposited on LaAlO_3 were investigated by *in situ* x-ray diffraction at the temperature range of 25–300 K, grazing incident x-ray diffraction, and high resolution x-ray diffraction. The nearly linear temperature dependence of the out-of-plane lattice constant of SrTiO_3 was observed in the measured temperature range. The depth distribution of the lattice strain at room temperature for SrTiO_3 films includes the surface layer, strained layer, and interface layer. © 2006 American Institute of Physics. [DOI: 10.1063/1.2424282]

SrTiO_3 (STO) is an incipient ferroelectric material in perovskite structure, which has been extensively studied for its application in tunable microwave devices for having a large and variable dielectric constant.^{1,2} STO is also a perfect prototype to investigate phase transition,³ especially to understand the surface and interface structural configuration for the perovskite films grown on it.⁴ Although ferroelectric properties were only reported through oxygen isotope exchange (ST^{18}O),^{3,5} and cation substitution,^{6,7} recent theories and experiments validate the existence of ferroelectricity in STO thin films under strain.^{8–10}

He *et al.*^{11–13} systematically studied the structural phase transition of STO thin films under strain. Devonshire¹⁴ predicted the shift of the ferroelectric phase transition temperature (T_c) for STO thin films due to the biaxial strain. Haeni *et al.*¹⁰ reported that the room temperature ferroelectricity appears for the tensile strained STO thin films on DyScO_3 substrates, although STO crystal is incipient ferroelectric. There is little work on the observation of distribution of lattice strain along the normal of sample surface for STO thin films.

In this letter, the distribution of the lattice strain of the epitaxial STO films grown on LaAlO_3 (LAO) (001) substrate by laser molecular beam epitaxy (MBE) deposition (L-MBE) is investigated. The temperature dependence of the c -direction lattice constant (c - T curve) is nearly linear, which is different from that of the bulk. The depth dependence of the lattice strain is not homogeneous, which may be due to the competition between the elastic restore and the lattice mismatch between STO film and LAO substrate.

STO films were grown on LAO (001) single crystal substrate in a L-MBE system. The technique was used to deposit STO on Si in our previous studies.^{15,16} Briefly, a single crystal STO target was used to grow STO film. A KrF excimer

laser was used in a repetition rate of 2 Hz. The substrate was heated to 770 °C. The film thicknesses were 80, 150, and 280 nm from the measurement of a Dektak³ ST surface profile. X-ray diffraction (XRD) ($\text{Cu K}\alpha$ radiation) analysis was performed using the $\theta/2\theta$ scan mode on a Rigaku Dmax-rB and a Bruker Advanced D8 X-ray diffractometer. The depth dependence of strain, which is related to the film thickness, was determined by grazing incident x-ray diffraction (surface x-ray diffraction), which was carried out on Bede D1 diffractometer. High resolution XRD was done on Siemens D5000HR.

Figure 1 shows a typical room temperature XRD $\theta/2\theta$ scan curve of STO films directly grown on (001) LAO. Only reflections of (001) from STO films and LAO substrate are observed. There are no extra XRD reflections from other crystalline orientations of STO films. The full width at half maximum (FWHM) of STO (002) peak is 0.32°. (The FWHM for the (002) rocking curve is 0.051° only, which is determined with high resolution x-ray diffraction.) In the inset of Fig. 1, the Φ scan of the (103) asymmetric reflection,

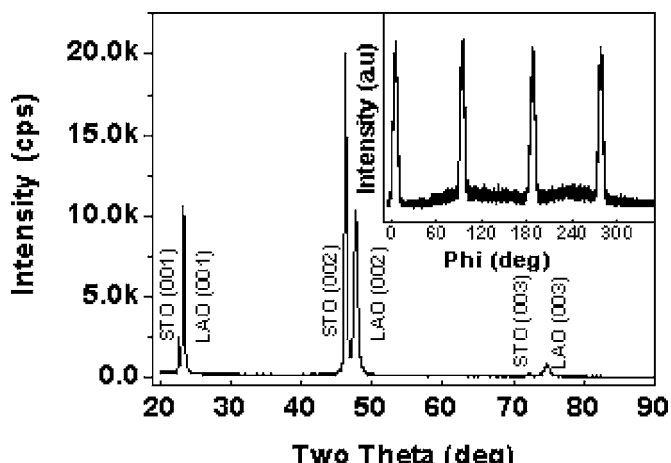


FIG. 1. X-ray diffraction patterns of STO thin film grown on LAO (100) substrates are shown. The inset shows the ϕ scan of the 280 nm STO film.

^{a)}Author to whom correspondence should be addressed; electronic mail: xswu@nju.edu.cn

^{b)}On leave from Department of Physics, The University of Hong Kong; electronic mail: apjhao@polyu.edu.hk

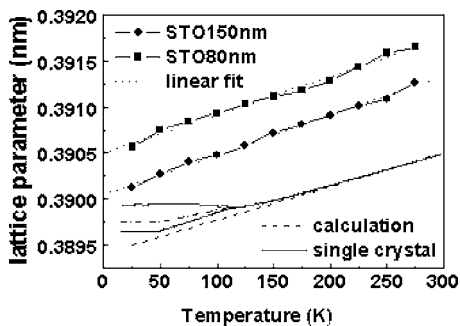


FIG. 2. Temperature dependence of out-of-plane lattice parameters for the samples with the STO films of 80 and 150 nm is shown. The solid line (Ref. 19) is the c - T curve for the bulk STO (the dash-dotted line is the cubic root of a unit cell volume). The linear dashed line is the calculated one (with the assumption of the thermal expansion coefficient of $9.4 \times 10^{-6}/\text{K}$).

for a STO film 280 nm thick deposited on LAO, is shown. Four peaks with almost equal intensity spaced by 90° are clearly shown and the typical FWHM is about 6.4° , which indicate that the film has high quality and is epitaxially grown on LAO substrate.

The temperature dependence of out-of-plane lattice parameter (c orientation) is obtained by *in situ* x-ray diffraction (Fig. 2). A nearly linear behavior of c versus temperature at the temperature range of 25–300 K is shown. The parameter c increases with the decrease of the thickness of STO film and is larger than that of the bulk at the same temperature, which indicates that a tetragonal distortion takes place. In comparison to the thermal expansion coefficients of the bulk STO of $9.4 \times 10^{-6}/\text{K}$ (Ref. 17) and LAO of $4.4 \times 10^{-6}/\text{K}$ (Ref. 18) at low temperature, individually, the fitted linear thermal expansion coefficients are $1.06 \times 10^{-5}/\text{K}$ and $1.11 \times 10^{-5}/\text{K}$ for the 80 and 150 nm thin films, which are almost consistent with that of the bulk. We can explain this phenomenon simply as follows: the relatively small difference in thermal expansion coefficient between the substrate and the film plays no role on thermal behavior of the film.

For bulk STO, the c - T curve has an abrupt change at the structural phase transition temperature (T_c). The c - T curve is almost linear above T_c , but as the temperature falls down, the lattice parameter splits at T_c because of domain formation and thus lattice relaxation.¹⁹ However, there is no change in the profile of c - T curve in the measured temperature range in our STO films. This observation is consistent with that reported by He *et al.*¹² It may be related to the substrate clamping effect rather than the lattice strain.

To determine the distribution lattice strain along the inner surface normal (i.e., the depth dependence of the lattice strain), grazing incidence x-ray diffraction or surface x-ray diffraction geometry was applied. The larger the grazing angle (χ) is, the deeper the x-ray penetration in the films is. We select (200) and (020) reflections to detect the in-plane lattice constant of the films. According to refraction principle, the angle of total reflection (α_c) can be calculated as $\alpha_c=0.315^\circ$ for STO, which is deduced from the following formula:²⁰

$$\alpha_c \approx \sqrt{\frac{N_A r_e \rho Z}{\pi A}} \lambda, \quad (1)$$

where N_A is Avogadro's constant, r_e the electronic classic radius, ρ the density of the material, Z the atomic number, A the molecular weight, and λ the wavelength of x-ray. The

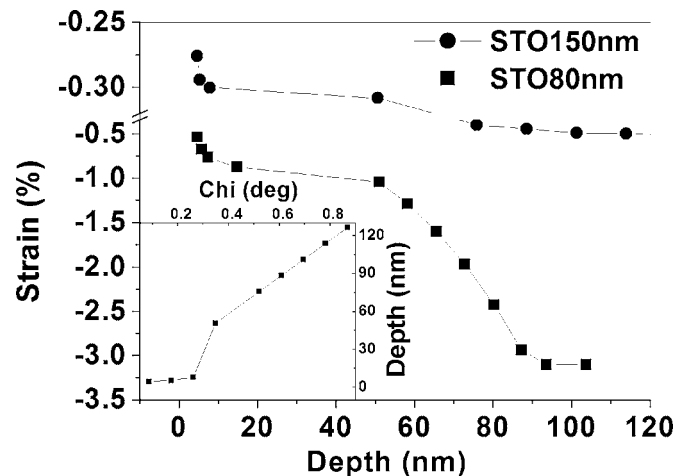


FIG. 3. Depth dependences of lattice strain of STO 150 and 80 nm thin films by using grazing incidence x-ray diffraction are shown. The inset gives the depth dependence of grazing incident angle.

maximum reflection is obtained at the grazing angle of 0.31° .

Figure 3 shows the depth dependence of the lattice strain for STO films. The penetration depth of x-ray in STO films is calculated by considering the process of the penetration for the electronic vector of electromagnetic wave at the interface. When the grazing incidence angle is less than the angle of total reflection ($\chi < \alpha_c$), the depth of x-ray penetration (L) follows the formula below:

$$L \approx \frac{\lambda}{2\pi\sqrt{\alpha_c^2 - \sin^2 \chi}}. \quad (2)$$

L has a minimal value of 45 Å for STO with $\lambda=1.5406$ Å. If grazing incidence angle is larger than the angle of total reflection ($\chi > \alpha_c$), the depth of penetration of x-ray (L) is approximately expressed as

$$L \approx \frac{1}{2\mu} \sin \chi, \quad (3)$$

where μ is the linear absorption coefficient of the material. For STO, $\mu=598.55 \text{ cm}^{-1}$. The maximal depth of penetration in our experiments is about 120 nm (with $\chi=0.85^\circ$) according to formula (3).

As we see in Fig. 3, the STO (150 nm) thin film remains relaxing within the detected depth of around 120 nm, with strain changes from -0.25% to -0.55% . This may indicate that the strain is mostly relaxed in the first 30 nm at the beginning of the film growth. This is proved by measuring the in-plane strain of STO (80 nm) thin film. The strain is relaxed in a large rate in the first 30 nm, which decreases from -3.1% (lattice mismatch) at the interface to about -0.81% at the depth of 50 nm from the surface (see also in Fig. 3). The results are in good agreement with both theory and other experiments.²¹ The competition between the elastic restore for STO unit cell and the lattice mismatch between STO film and LAO substrate may result in the distribution of lattice strain in films.

From the curves of the dependence of lattice strain for the samples of 150 and 80 nm STO thin films, we may deduce that the depth distribution of the lattice strain includes the surface layer, strained layer, and interface layer, which is consistent with our previous studies on $\text{La}_{2/3}\text{Ca}_{1/3}\text{MnO}_3$ films on the STO substrates.²² The surface layer, where the

lattice strain varies sharply, is about 8 nm from the film surface for both of the samples, which may result from the surface tension. The lattice strain varies slowly in the depth from about 8 to about 50 nm for the sample of 80 nm STO film and to about 120 nm for the sample of 150 nm STO film, respectively. This may be due to the relaxation of strain in the surface layer. In the deeper layer, the strain increases with the increase of the depth. This can be seen in the curve of 80 nm STO film. Unfortunately, we cannot observe the larger variation in lattice strain in the depth range from 120 to 150 nm (the last 30 nm) for the sample of 150 nm STO film due to the limitation of the experiments. The films are not fully relaxed, even for the film with a thickness of 280 nm as observed in our measurement, which are quite similar to that reported by other groups.²¹

In summary, a nearly linear temperature dependence of the out-of-plane lattice constant for STO films deposited on LAO substrate is observed in the temperature range of 25–300 K by *in situ* x-ray diffraction. The lattice strain distribution for STO on LAO along the surface normal direction is inhomogeneous, which can be divided into three sublayers with different lattice strains, i.e., the surface layer, strained layer, and interface layer.

This work has been supported by NNSFC (Grant Nos. 10474031 and 10523001). The authors would like to thank the State Key Project of Fundamental Research (Grant No. 001CB610602, 2006CB0L1002). Two of the authors (J.H.H. and J.G.) acknowledge the Research Grants Council of Hong Kong for grants (Project Nos. PolyU 7025/04P and PolyU 7025/05P).

¹X. X. Xi, H. C. Li, W. Si, A. A. Sirenko, I. A. Akimov, J. R. Fox, A. M. Clark, and J. Hao, *J. Electroceram.* **4**, 393 (2000).

²Wontae Chang, Steven W. Kirchoefer, Jeffrey A. Bellotti, Syed B. Qadri,

and Jeffrey M. Pond, *J. Appl. Phys.* **98**, 024107 (2005).

³Robert Blinc, Bošjan Zalar, Valentin V. Laguta, and Mitsuru Itoh, *Phys. Rev. Lett.* **94**, 147601 (2005).

⁴Naoyuki Nakagawa, Harold Y. Hwang, and David A. Muller, *Nature (London)* **5**, 204 (2006).

⁵M. Itoh, R. Wang, Y. Inaguma, T. Yamaguchi, Y.-J. Shan, and T. Nakamura, *Phys. Rev. Lett.* **82**, 3540 (1999).

⁶A. Durán, E. Martínez, J. A. Díaz, and J. M. Siqueiros, *J. Appl. Phys.* **97**, 104109 (2005).

⁷V. B. Shirokov, V. I. Torgashev, and A. A. Bakirov, *Phys. Rev. B* **73**, 104116 (2006).

⁸T. Yamada, J. Petzelt, A. K. Tagantsev, S. Denisov, D. Noujini, P. K. Petrov, A. Mackova, K. Fujito, T. Kiguchi, K. Shinozaki, N. Mizutani, V. O. Sherman, P. Muralt, and N. Setter, *Phys. Rev. Lett.* **96**, 157602 (2006).

⁹Oleg Tikhomirov, *Phys. Rev. Lett.* **89**, 147601 (2002).

¹⁰J. H. Haeni, P. Irvin, W. Chang, R. Uecker, P. Reiche, Y. L. Li, S. Choudhury, W. Tian, M. E. Hawley, B. Craig, A. K. Tagantsev, X. Q. Pan, S. K. Streiffer, L. Q. Chen, S. W. Kirchoefer, J. Levy, and D. G. Schlom, *Nature (London)* **430**, 758 (2004).

¹¹Feizhou He, B. O. Wells, S. M. Shapiro, M. v. Zimmermann, A. Clark, and X. X. Xi, *Appl. Phys. Lett.* **83**, 123 (2003).

¹²Feizhou He, B. O. Wells, Z.-G. Ban, S. P. Alpay, S. Grenier, S. M. Shapiro, Weidong Si, A. Clark, and X. X. Xi, *Phys. Rev. B* **70**, 235405 (2004).

¹³Feizhou He, B. O. Wells, and S. M. Shapiro, *Phys. Rev. Lett.* **94**, 176101 (2005).

¹⁴A. F. Devonshire, *Philos. Mag., Suppl.* **3**, 85 (1954).

¹⁵J. H. Hao, J. Gao, Z. Wang, and D. P. Yu, *Appl. Phys. Lett.* **87**, 131908 (2005).

¹⁶J. H. Hao, J. Gao, and H. K. Wong, *Appl. Phys. A: Mater. Sci. Process.* **81**, 1233 (2005).

¹⁷Farrel W. Lytle, *J. Appl. Phys.* **35**, 2212 (1964).

¹⁸B. C. Chakoumakos, D. G. Schlom, M. Urbanik, and J. Luine, *J. Appl. Phys.* **83**, 1979 (1998).

¹⁹A. Okazaki and M. Kawaminami, *Mater. Res. Bull.* **8**, 545 (1973).

²⁰H. Dosch, *Phys. Rev. B* **35**, 2137 (1987).

²¹L. S.-J. Peng, X. X. Xi, B. H. Moeckly, and S. P. Alpay, *Appl. Phys. Lett.* **83**, 4592 (2003).

²²X. S. Wu, H. L. Cai, J. Xu, W. S. Tan, A. Hu, S. S. Jiang, T. P. A. Hase, B. K. Tanner, and G. Xiong, *J. Appl. Phys.* **95**, 7109 (2004).